

# Four complementary theoretical approaches for the analysis of NMR paramagnetic relaxation

Nathaniel Schaeffe, Robert Sharp \*

*Department of Chemistry, The University of Michigan, Ann Arbor, MI 48109, USA*

Received 27 January 2005; revised 12 May 2005

Available online 11 July 2005

## Abstract

Four theoretical and computational approaches used at the University of Michigan to analyze NMR paramagnetic relaxation enhancement (NMR-PRE) are described. The primary objective of the theory is to describe the relationship of the NMR-PRE phenomenon to the electron spin hamiltonian and the spin energy level structure when zero field splitting interactions are significant. Four formulations of theory are discussed: (1) spin dynamics simulation; (2) the laboratory frame “constant  $H_S$ ” formulation; (3) the Molecular Frame “constant  $H_S$ ” formulation; and (4) the zfs-limit “constant  $H_S$ ” formulation. No single theoretical approach describes all important aspects of the relaxation mechanism in a fully satisfactory way. We use the four formulations in a complementary manner to provide as complete a picture of the relaxation mechanism as possible. We also discuss the integration of NMR-PRE theory and recently developed theory of electron spin relaxation which accounts for effects of the permanent zfs hamiltonian. © 2005 Elsevier Inc. All rights reserved.

*Keywords:* NMR relaxation; Paramagnetic NMR relaxation; Zero field splitting

## 1. Introduction

For a number of years, we have been interested in NMR relaxation induced by  $S > 1/2$  paramagnetic metal ions in solution. Dipole–dipole coupling of the nuclear magnetic moment,  $\vec{\mu}_I$ , and the dipolar field of unpaired electron spin,  $\vec{B}_S$ , provides a highly efficient pathway for NMR relaxation, so that millimolar or lower concentrations of metal ion will frequently provide the principal relaxation mechanism for solvent protons. Paramagnetic NMR relaxation enhancement (NMR-PRE) involves an exchange of energy between the nuclear ( $I$ ) and electron ( $S$ ) spins, a process that is dependent on the resonant coupling of  $\vec{B}_S$  and  $\vec{\mu}_I$ . Because of the resonance requirement, the relaxation mechanism depends intimately on the motions, both coherent and stochastic, of the electron spin vector. The physical

situation is relatively simple for  $S = 1/2$  ions, for which the spin motion is driven by the electronic Zeeman hamiltonian ( $H_{Zeem}$ ) plus, when it is present, the nuclear–electron hyperfine hamiltonian ( $H_{hf}$ ). For  $S \geq 1$ , the situation is considerably more complicated because of presence of permanent zero-field splitting (zfs) interactions,  $H_{zfs}^0$ .  $H_{zfs}^0$  and  $H_{Zeem}$  are often of roughly comparable magnitude; in common laboratory experiments,  $H_{zfs}^0$  may be larger or smaller than  $H_{Zeem}$  depending on the metal ion and laboratory field strength. When  $H_{zfs}^0 \geq H_{Zeem}$ ,  $H_{zfs}^0$  exerts a critical influence on the electron spin motion and spatial quantization, which in turn profoundly affects the NMR-PRE.

During the past 10 years, our laboratory has studied various aspects of these phenomena theoretically and experimentally [1–13] with the objective of understanding the relationship of the NMR-PRE phenomenon to the electron spin level diagram and the electron spin motion. Systematic studies of this relationship have also been published by the laboratories of Kowalewski and

\* Corresponding author. Fax: +1 734 649 4865.

E-mail address: [rrsharp@umich.edu](mailto:rrsharp@umich.edu) (R. Sharp).

Westlund in Sweden [14–16] and Kruk in Germany [17]. Experimental information concerning the physical mechanism of NMR-PRE is derived primarily from the analysis of magnetic relaxation dispersion (MRD) profiles, in which the NMR relaxation rate of solvent protons in paramagnetic solutions is measured as a function of laboratory magnetic field strength across a broad range (several orders of magnitude) of field variation. A plot of proton  $R_1$  vs field strength (the MRD profile) is typically measured between about  $10^{-4}$  and 2 T. For  $S \geq 1$  ions, the low end of this range corresponds to the zfs-limit ( $H_{zfs}^0 > H_{Zeem}$ ), where the spatial quantization of the electron spin motion is aligned along molecule-fixed coordinate axes, and the frequencies of the coherent spin oscillations are determined by the splittings of the zfs level diagram. (This assumes that Brownian reorientation is not sufficiently rapid to motionally average to zero the level structure of  $H_{zfs}^0$ .) The opposite limit is that of high laboratory field strength (the Zeeman-limit,  $H_{Zeem} > H_{zfs}^0$ ), where  $\langle \vec{S} \rangle$  executes a Larmor precession that is spatially quantized along the field direction. This limit may or may not be reached experimentally depending on the metal ion and spin state and the magnitude of the zfs. In the intermediate regime ( $H_{zfs}^0 \approx H_{Zeem}$ ), the spin motion is complex and lacks well-defined spatial quantization. Further complicating the situation is the fact that the permanent electron spin hamiltonian

$$H_S(\alpha, \beta, \gamma, t) = H_{Zeem} + H_{zfs}^0(\alpha, \beta, \gamma, t), \quad (1)$$

depends on molecular orientation  $(\alpha, \beta, \gamma)$  and is explicitly time-dependent due to Brownian reorientation. When  $H_{zfs}^0(\alpha, \beta, \gamma, t) \geq H_{Zeem}$ , the zero-order electron spin wavefunctions are stochastic functions of time, which greatly complicates the calculation.

The MRD profile depends on chemical and physical parameters relating to both the  $I$ – $S$  dipole–dipole hamiltonian ( $H_{IS}$ ), which mediates energy transfer between the spin systems, and the electron spin hamiltonian ( $H_S$ ), which drives the coherent motions of  $S$ . The form of the MRD profile depends intimately on the electron spin quantum number (the profiles for  $S = 1, 3/2, 2, 5/2$  all exhibit major characteristic differences [2,6,10,14]) as well as on the structure of the spin level diagram and the detailed form of the zfs tensor. In particular, there is a surprisingly strong dependence on the low-symmetry components of the zfs tensor, i.e., on the orthorhombic zfs term  $E$  for  $S = 1$  [3,5,6,10,18,19], and on the tetragonal fourth-order zfs term for  $S \geq 2$  [5,11,13]. Our principal interest lies in understanding the relationship of NMR-PRE to the electron spin level diagram.

This paper describes four theoretical approaches currently used at Michigan to analyze NMR paramagnetic relaxation enhancement. These are: (1) spin dynamics (SD) simulation [20–22], (2) the “constant  $H_S$ ” LF

(laboratory frame) formulation, (3) the “constant  $H_S$ ” MF (molecular frame) formulation, and (4) the “constant  $H_S$ ” zfs-limit formulation [5]. These four formulations are implemented in a computer program, Parelax2, which has evolved from an earlier program, Parelax [23]. A program similar to Parelax has been developed by Bertini et al. [24] in Florence. The algorithms of Parelax2 and Parelax are based on quite different theoretical formulations, and much additional functionality has been added to the former.

We use the four approaches in a complementary manner to provide as full a picture of the relaxation mechanism as possible. Each approach has advantages and drawbacks, none providing an entirely satisfactory description of the relaxation process. SD simulation provides a realistic description of the role of Brownian reorientation on the spin motions and the  $I$ – $S$  dipole–dipole coupling, which the “constant  $H_S$ ” formulations do not. Thus the latter do not describe NMR-PRE quantitatively when Brownian reorientation is an important contributor to the dipolar correlation time.

The principal advantage of “constant  $H_S$ ” is that these formulations, unlike SD, provide a physically transparent description of the relaxation mechanism in terms of the contributions of specific spin matrix elements (for example,  $\langle S_z \rangle$ ). Physical transparency requires that the formulation be cast in a coordinate frame corresponding to the spatial quantization of the electron spin motion. It is for this reason that we use either LF or MF formulations of “constant  $H_S$ ” theory according to whether the electron spin system is in the vicinity of the Zeeman- or zfs-limit.

A simple example of the kind of interpretation meant is provided by the Zeeman-limit situation, where  $\langle S_z \rangle$  is a constant of the motion. The dipolar power band associated with  $\langle S_z \rangle$  is centered at zero frequency. In contrast, the non-vanishing matrix elements of  $\langle S_x \rangle$  oscillate at the electron Larmor frequency ( $\omega_S$ ), and the associated dipolar power band is centered at  $\omega_S$ . NMR  $R_1$  relaxation depends on resonant coupling between the  $I$  and  $S$  spins, and thus the relaxation efficiency depends on the low frequency motions ( $\omega \approx \omega_I$ ) of the  $I$ – $S$  dipolar power spectrum. In the Zeeman-limit,  $\langle S_z \rangle$  is usually the main contributor to the NMR-PRE, except at low field strengths where the dipolar power band of  $\langle S_x \rangle$  significantly overlaps  $\omega_I$ .

The zfs-limit and intermediate regimes of field strength present many fascinating connections between the spin level diagram and the NMR-PRE. For  $S \geq 2$ , quite subtle level splittings [11] and wavefunction mixing [13] arising from low symmetry fourth-order zfs components can determine the form of the MRD profile. Physical interpretations of these phenomena are possible within the “constant  $H_S$ ” formulations when the coordinate frame matches that of the spatial quantization of the spin motion. It is for this reason that we use both

LF and MF formulations of theory. The fullest picture of the spin physics is obtained when the four formulations are used in a complementary way. (It should be recognized that LF and MF formulations are not approximations valid only in the Zeeman- and zfs-limits; rather, they give identical numerical results for  $R_{1M}$  in all regimes of field strength as long as electron spin relaxation is treated equivalently.)

The theoretical approaches implemented by Parelax2 differ from traditional approaches in that they emphasize the use of operators for the local dipolar field of  $S$ . These quantities are especially convenient for transforming the problem between the LF and MF and for using different coordinate frames to describe the electron and nuclear spin motions. Prior descriptions of the four formulations are incomplete and, in some cases, they differ from their current implementation in Parelax2. A unified description of the theory that clearly shows the relationship of the various formulations to each other and the assumptions underlying each is needed and is provided here. We also discuss in some detail the integration of NMR-PRE theory with recently developed theory of electron spin relaxation, a topic which involves several subtleties.

## 2. General formulation of the problem

In MRD, paramagnetic enhancement of the solvent  $R_1$  by a metal ion is mediated by chemical exchange reactions, which transfer relaxed nuclear spins (usually water protons) between the metal coordination sphere and the pool of unbound solvent. When the bound mole fraction ( $f_M$ ) is small, the NMR-PRE is given by [25]

$$R_{1p} = f_M / (T_{1M} + \tau_M), \quad (2)$$

where  $T_{1M} (= R_{1M}^{-1})$  is the relaxation time in the bound site, and  $\tau_M$  is the chemical exchange residence time. The Zeeman-limit (SBM) theory of  $R_{1M}$  is well known [26–28]. In this and the following section, we develop theory which incorporates the electron spin hamiltonian of Eq. (1), where  $H_{zfs}^0$  has arbitrary form and magnitude.

From the linear response theory of Kubo and Tomita [29,30], the  $T_1$  NMR relaxation rate is given by,

$$R_{1M} = (2\hbar^2)^{-1} 3^1 (I(I+1))^{-1} \times \int_{-\infty}^{\infty} \exp(i\omega_I t) \{ \langle I_z, H'_{IS}(t) [H'_{IS}(0), I_z] \rangle \}_{\text{ea}} dt, \quad (3a)$$

$$H'_{IS} = \exp(i\omega_I t) H_{IS} \exp(-i\omega_I t), \quad (3b)$$

where  $\omega_I$  is the nuclear Larmor frequency. The angle brackets denote traces over the spin variables of  $I$  and  $S$ , and the braces denote an ensemble average over molecular degrees of freedom.  $H_{IS}$  is the nuclear–electron ( $I$ – $S$ ) dipole–dipole hamiltonian, which is given in spherical tensor form in Appendix A. For our purposes,

it is useful to write  $H_{IS}$  in a somewhat different form as an interaction of the nuclear magnetic moment,  $\vec{\mu}_I$ , with the local dipolar field operator,  $\vec{B}_S$ , of  $S$ :

$$H_{IS} = -\vec{\mu}_I \cdot \vec{B}_S, \quad (4a)$$

$$= -\gamma_I \hbar \sum_{m=-1}^{+1} (-1)^m I_m^{(1)} B_{-m}^{(1)}. \quad (4b)$$

Eq. (4b) is written in spherical tensor form, e.g.,

$$I_0^{(1)} = I_z, \quad (5a)$$

$$I_{\pm 1}^{(1)} = \mp 2^{-1/2} I_{\pm}, \quad (5b)$$

and  $B_m^{(1)}$  are the spherical tensor components of  $\vec{B}_S$ . The utility of Eq. (4b) lies in the fact that  $I$  and  $S$  have different spatial quantization when  $H_{zfs}^0 > H_{Zeem}$ , and this form of  $H_{IS}$  is convenient for expressing  $\vec{\mu}_I$  and  $\vec{B}_S$  in their natural coordinate systems. The quantum mechanical operator that describes  $\vec{B}_S$  can be constructed as a first-rank tensor by contracting the electron spin spherical tensor,  $S^{(1)}$ , with the second-rank spherical harmonics,  $Y_m^{(2)}(\theta, \varphi)$ , the arguments of which are the polar angles that specify the orientation of the interspin vector,  $\vec{r}_{IS}$ , with respect to the laboratory magnetic field,  $\vec{B}_0$ :

$$B^{(1)} = c_B \{ S^{(1)} \otimes Y^{(2)} \}^{(1)}, \quad (6a)$$

$$B_m^{(1)} = 3^{1/2} c_B \sum_{p=-1}^{+1} (-1)^{1-m} \begin{pmatrix} 1 & 2 & 1 \\ p & m-p & -m \end{pmatrix} \times S_p^{(1)} Y_{m-p}^{(2)}(\theta, \varphi), \quad (6b)$$

$$c_B = -(8\pi)^{1/2} g_e \beta_e r_{IS}^{-3} (\mu_0/4\pi), \quad (6c)$$

where  $g_e$ ,  $\beta_e$ , and  $\mu_0$  are the electron  $g$ -value, Bohr magneton, and vacuum permeability, and  $m = 0, \pm 1$ . Specific forms of the field operators,  $B_m^{(1)}$ , are given in Appendix B. These quantities can be defined in either a laboratory-fixed (LF) or molecule-fixed (MF) coordinate frame as is convenient to describe the motions of  $\langle \vec{S} \rangle$ . We proceed with the LF formulation, but for the MF formulations, we will use the MF expression for  $H_{IS}$ .

Inserting Eq. (4b) into Eq. (3a) gives

$$R_{1M} = (2\hbar^2)^{-1} 3 [I(I+1)]^{-1} \sum_{m,m'=-1}^{+1} (-1)^{m+m'} \times \langle [I_0^{(1)}, I_m^{(1)}] [I_{m'}^{(1)}, I_0^{(1)}] \rangle \int_{-\infty}^{+\infty} dt \exp(i\omega_I t) \times \left\{ \langle B_{-m}^{(1)}(t) B_{-m'}^{(1)}(0) \rangle_S \right\}_{\text{ea}}. \quad (7)$$

The commutators can be evaluated using Racah's relations,

$$[I_0^{(1)}, I_m^{(1)}] = m I_m^{(1)}, \quad (8)$$

and the trace over the variables of  $I$  becomes

$$-(mm')\langle I_m^{(1)} I_{m'}^{(1)} \rangle_I = -(mm')3^{-1}I(I+1)\delta_{m+m'}\delta_{m^2-1}, \quad (9)$$

which vanishes unless  $m = -m' = \pm 1$ . The expression for  $R_{1M}$  becomes

$$R_{1M} = -\gamma_I^2 \int_{-\infty}^{+\infty} dt \exp(i\omega_I t) \text{Re} \left\{ \left\langle B_{+1}^{(1)}(t) B_{-1}^{(1)}(0) \right\rangle_S \right\}_{\text{ca}}. \quad (10)$$

The TCFs of the dipolar field can be evaluated from Eqs. (6a)–(6c) to give

$$\begin{aligned} \langle B_{+1}^{(1)}(t) B_{-1}^{(1)}(0) \rangle &= 24\pi g_e^2 \beta_e^2 r_{IS}^{-6} \left( \frac{\mu_0}{4\pi} \right)^2 \\ &\times \sum_{p,p'=-1}^{+1} \begin{pmatrix} 1 & 2 & 1 \\ p & (1-p) & -1 \end{pmatrix} \begin{pmatrix} 1 & 2 & 1 \\ p' & (-1-p') & 1 \end{pmatrix} \\ &\times \left\langle S_p^{(1)}(t) S_{p'}^{(1)}(0) \right\rangle_S Y_{1-p}^{(2)}(\theta, \varphi; t) Y_{-1-p'}^{(2)}(\theta, \varphi; 0). \end{aligned} \quad (11)$$

In this LF formulation, a further transformation of the spherical harmonic functions is desirable, since these functions are fixed in the MF. The transformation can be accomplished by expanding the LF spherical harmonics in terms of MF functions (denoted by a karat)

$$Y_q^{(2)}(\theta, \varphi) = \sum_{q'=-2}^2 Y_{q'}^{(2)}(\hat{\theta}, \hat{\varphi}) D_{q',q}^{(2)}(\alpha, \beta, \gamma), \quad (12)$$

where  $D_{q',q}^{(2)}(\alpha, \beta, \gamma)$  are Wigner rotation matrix elements and  $(\alpha, \beta, \gamma)$  are the Euler angles which rotate the MF to the LF.

Inserting Eqs. (11) and (12) into Eq. (10) gives the following LF expression for  $R_{1M}$ ,

$$\begin{aligned} R_{1M} &= -48\pi(\gamma_I g_e \beta_e)^2 r_{IS}^{-6} (\mu_0/4\pi)^2 \\ &\times \sum_{p,p'=-1}^1 \left\{ \begin{matrix} 1 & 2 & 1 \\ p & (1-p) & -1 \end{matrix} \right\} \left\{ \begin{matrix} 1 & 2 & 1 \\ p' & (-1-p') & 1 \end{matrix} \right\} \\ &\times \text{Re} \left( \sum_{q,q'=-2}^2 Y_q^{(2)}(\hat{\theta}, \hat{\varphi}) Y_{q'}^{(2)}(\hat{\theta}, \hat{\varphi}) \right. \\ &\times \int_0^\infty dt e^{i\omega_I t} \left\{ \left\langle S_p^{(1)}(t) S_{p'}^{(1)}(0) \right\rangle_S \exp(-t/\tau_M) \right. \\ &\left. \left. \times D_{q,1-p}^{(2)}(\alpha, \beta, \gamma; t) D_{q',-1-p'}^{(2)}(\alpha, \beta, \gamma; 0) \right\}_{\text{ca}} \right) \end{aligned} \quad (13)$$

in which all of the variables are defined in the LF except  $(\hat{\theta}, \hat{\varphi})$ . A phenomenological decay function,  $\exp(-t/\tau_M)$ , has been inserted in the integrand to describe the interruption of  $I$ - $S$  dipolar coupling due to chemical exchange.

### 3. Electron spin relaxation

The spin TCFs,

$$G_{p,p'}(t) = \left\langle S_p^{(1)}(t) \cdot S_{p'}^{(1)}(0) \right\rangle, \quad (14)$$

describe both the coherent oscillations and thermal relaxation of  $\langle S \rangle$ . To evaluate these quantities,  $S_p^{(1)}(t)$  is written in the Heisenberg representation,

$$S_p^{(1)}(t) = U^\dagger(t) S_p^{(1)} U(t), \quad (15a)$$

$$U(t) = \exp(-iH_S(\alpha, \beta, \gamma, t)t/\hbar), \quad (15b)$$

$$H_S(\alpha, \beta, \gamma, t) = H_{Z\text{cem}} + H_{zfs}^0(\alpha, \beta, \gamma, t) + H_{zfs}^c(t) + H_{zfs}^v(t). \quad (16)$$

The stochastic time dependence of  $H_S(\alpha, \beta, \gamma; t)$  produces the thermal relaxation of  $S$  and arises from three physical processes, namely: (1) Brownian reorientation of the zfs tensor axes (represented by  $H_{zfs}^0(\alpha, \beta, \gamma; t)$ ), (2) collisional modulation of the zfs tensor components ( $H_{zfs}^c(t)$ ), and (3) zfs modulation by vibrational damping [31] ( $H_{zfs}^v(t)$ ). These three degrees of freedom are approximately independent, and their relaxation contributions are taken to be additive. The vibrational relaxation mechanism has been neglected by most (but not all [32,33]) authors, and Parelax2 neglects it as well.

The reorientational zfs mechanism is described implicitly in SD simulations but is ignored in all of the “constant  $H_S$ ” formulations, which neglect the time dependence of  $H_{zfs}^0$ . This mechanism is discussed further in Section 4.1 and in [22].

The collisional zfs mechanism arises from the stochastic motions of  $H_{zfs}^c(t)$ , a hamiltonian of zero trace that describes the distortion of the zfs tensor during intermolecular collisions. Detailed dynamic modeling of these motions within a theory of NMR relaxation is difficult because of the complexity of the molecular force fields and the complex relationship of nuclear motions to the motion of the zfs tensor, as is illustrated by the first-principles calculations for  $\text{Ni}(\text{H}_2\text{O})_6^{2+}$  of Odellius et al. [34,35]. Further complicating the description is the wide range of time-scales in the problem. Redfield Theory, which assumes that the correlation time,  $\tau_v$ , for zfs distortion is short compared to the relaxation time,  $\tau_S$ , is not always appropriate when  $\tau_S$  is very short. Considerable progress on a non-Redfield theory has been made within the SLE formalism by modeling the distortion process as a pseudorotation [16,36–38]. A Monte Carlo approach to the non-Redfield calculation has also been reported by Rast et al. [39]. Within the Redfield approximation, quite simple zfs-limit expressions for  $\tau_S$  (defined in the MF) have been derived by Westlund [40] for the spin-1 case. Bertini et al. [41] subsequently generalized these results to non-Redfield situations using SLE. Detailed Redfield calculations of ESR



linewidths of the  $S = 7/2$  ion Gd(III) have been reported by Rast et al. [42,43], whose treatment included the effects of cylindrical fourth-order zfs terms. Gd(III) is especially interesting chemically because of research concerning the use of Gd complexes as MRI contrast agents.

Parela2 describes electron spin relaxation using the theory of Sharp [44], which calculates the electron spin relaxation times in NMR experiments, where the electron spin hamiltonian is at thermal equilibrium. This theory accounts for the effects of  $H_{zfs}^0$  and is valid for all  $S$ , subject to the Redfield approximation. The integration of the NMR and electron spin relaxation theories is discussed in Section 5. The following three options are provided by Parela2: (1) field-independent parameters,  $\tau_{SX(Y,Z)}$ , can be entered; (2)  $\tau_{S,r}$  can be calculated using the well known Zeeman-limit theory of Bloembergen and Morgan (BM) [28]; (3)  $\tau_{S,r}$  can be calculated using the theory of [44] (see Section 5).

#### 4. The four formulations of theory

This section describes the four formulations of NMR-PRE theory used by Parela2, thus continuing the development of Section 2. Section 5 discusses the integration of the theoretical descriptions of NMR and electron spin relaxation.

##### 4.1. Spin dynamics simulation

Spin dynamics simulations [20–22] evaluate the TCF of Eq. (14) in the time domain as an ensemble average of Brownian trajectories of the spin motion, using the hamiltonian of Eq. (1) to calculate the propagator of Eqs. (15b). SD simulation describes the influence of the reorientation of the zfs principal axes on the electron spin motion, and thus SD calculates the zfs-reorientational contribution to electron spin relaxation directly. The effects of  $H_{zfs}^c(t)$  (the collisional mechanism) are incorporated in the form of an exponential factor in  $G_{p,p'}(t)$  as described above and in Section 5.

We outline the SD algorithms briefly here (see also [22]). Molecular reorientation is modeled as a classical random-walk, following the work of Ivanov [45], in which molecular reorientation is comprised of a stochastic sequence of rotational jumps separated by random intervals. The rotation axis of each jump is randomly oriented in space. The jump angles are distributed randomly as a Gaussian deviate of zero mean and a width  $\sigma_\phi$ . Thus the molecular motion is described as a thermal ensemble of trajectories, each consisting of a sequence of intervals of random duration,  $(t_1, t_2, t_3, \dots)$ , in which molecular orientation is fixed, connected by sudden rotational jumps. The propagator of Eqs. (15b) can be decomposed as follows

$$U(t, t_0) = U^{(0)}(t_1, t_0)U'(t_1), U^{(1)}(t_2, t_1)U'(t_2) \cdots U^{(n)}(t, t_n), \quad (17)$$

where  $U^{(n)}(t, t_n)$  is the propagator in the interval  $\tau_n \rightarrow \tau_{n+1}$ , and  $U'(t_n)$  is the propagator for the jump connecting the intervals,  $n$  and  $n+1$ . If it is assumed that jumps are rapid compared to the inverse transition frequencies of  $H_S$ , the state vector is unaffected (this is the ‘‘Sudden Approximation’’ [46,47])

$$U'(t_n) = \underline{1}. \quad (18)$$

After the  $n$ th reorientational jump in a trajectory, the Wigner rotation matrix elements in Eq. (13) and the spin Hamiltonian in Eq. (16) are re-evaluated. The spin propagator,

$$U(t, t_n) = \exp(-iH_S(t - t_n)/\hbar), \quad (19)$$

is then evaluated from the series definition and used to propagate the spin variables across the time interval,  $(t_n \rightarrow t_{n+1})$ . In this way, trajectories of the  $G_{p,p'}(t)$  are computed across a total time interval which is chosen to be sufficiently long to ensure the decay of the TCF. The number of time steps in a trajectory depends on the physical situation: it can range from as few as 30 when electron spin relaxation is rapid compared to the coherent spin oscillations to several thousand in opposite case. In all cases, the time interval between adjacent jumps must be short enough to describe the fastest oscillations of the spin motion, and the total duration of the simulation must be long enough to describe the thermal decay of the TCF.

Propagation of the spin operators is carried out in the LF. Therefore SD is an LF formulation, which requires that electron spin relaxation be defined in the LF rather than the MF (see Section 5.1). Because SD is a time-domain formulation, it cannot incorporate eigenstate-specific electron spin relaxation times. Referring to the discussion of Section 5, SD can incorporate the relaxation times,  $\tau_{S1,2}$ , of BM Theory; also, the eigenstate-averaged relaxation times,  $\tau_{S,r}$ , of [44]; but not eigenstate-specific relaxation times,  $\tau_{S,r}^{(\mu)}$ , or relaxation times,  $\hat{\tau}_{S,r}$ , and  $\hat{\tau}_{S,r}^{(\mu)}$ , defined in the MF.

##### 4.2. The LF ‘‘constant $H_S$ ’’ formulation

The ‘‘constant  $H_S$ ’’ formulations ignore reorientation of the zfs principal axes, with the result that  $H_{zfs}^0(\alpha, \beta, \gamma; t)$  is taken to be time-independent as in a powder,

$$H_S(\alpha, \beta, \gamma, t) = H_{Zeem} + H_{zfs}^0(\alpha, \beta, \gamma) + H_{zfs}^c(t), \quad (20a)$$

$$= H_S^0(\alpha, \beta, \gamma) + H_{zfs}^c(t). \quad (20b)$$

The static hamiltonian,  $H_S^0(\alpha, \beta, \gamma)$ , drives the coherent spin oscillations, and  $H_{zfs}^c(t)$  is the stochastic hamiltonian which drives electron spin relaxation. In this

approximation, the theory simplifies considerably, since the spin eigenfunctions are time-independent, and the TCFs of Eq. (14) can be evaluated in closed form. Expressing  $G_{p,p'}(t)$  as a trace, we have

$$G_{p,p'}(t) = \text{Tr} \left[ \rho_S^0 \left\langle \exp(iH_S(t)/\hbar) S_p^{(1)} \right. \right. \\ \left. \left. \times \exp(-iH_S(t)/\hbar) S_{p'}^{(1)}(0) \right\rangle \right] \\ = (2S+1)^{-1} \sum_{\mu, \nu} \langle \mu | S_p^{(1)} | \nu \rangle \langle \nu | S_{p'}^{(1)} | \mu \rangle \\ \times \exp \left( -i \left[ \omega_{\mu\nu} - 1/\tau_{S,p}^{(\mu)} \right] t \right), \quad (21)$$

where  $\{\mu, \nu\}$  are eigenvectors of  $H_S^0(\alpha, \beta, \gamma)$  and  $\omega_{\mu, \nu}$  are eigenfrequencies. The electron spin density matrix,  $\rho_S^0$ , is diagonal in NMR experiments. We further assume the high-temperature limit, where

$$\rho_S^0 = (2S+1)^{-1} \mathbf{1}. \quad (22)$$

Inserting these results into Eq. (13) and evaluating the integral gives the following LF “constant  $H_S$ ” expression for  $R_{1M}$ :

$$R_{1M} = -48\pi(\gamma_I g_e \beta_e)^2 r_{IS}^{-6} (\mu_0/4\pi)^2 \\ \times \sum_{p,p'=-1}^1 \left\{ \begin{matrix} 1 & 2 & 1 \\ p & (1-p) & -1 \end{matrix} \right\} \left\{ \begin{matrix} 1 & 2 & 1 \\ p' & (-1-p') & 1 \end{matrix} \right\} \\ \times \sum_{q,q'=-2}^2 Y_q^{(2)}(\hat{\theta}, \hat{\phi}) Y_{q'}^{(2)}(\hat{\theta}, \hat{\phi}) \\ \times \left\{ D_{q,1-p}^{(2)}(\alpha, \beta, \gamma) D_{q',-1-p'}^{(2)}(\alpha, \beta, \gamma) \right. \\ \left. \times (2S+1)^{-1} \sum_{\mu, \nu} \langle \mu | S_p^{(1)} | \nu \rangle \langle \nu | S_{p'}^{(1)} | \mu \rangle j_p^{(\mu)}(\omega_{\mu\nu}) \right\}_{\text{ea}}, \quad (23a)$$

$$j_p^{(\mu)}(\omega_{\mu\nu}) = \frac{\tau_{d,p}^{(\mu)}}{1 + (\omega_I - \omega_{\mu\nu})^2 (\tau_{d,p}^{(\mu)})^2}, \quad (23b)$$

$$(\tau_{d,p}^{(\mu)})^{-1} = (\tau_R^{(2)})^{-1} + (\tau_{S,p}^{(\mu)})^{-1} + (\tau_M)^{-1}. \quad (23c)$$

The dipolar correlation rate of Eq. (23c) has contributions from Brownian reorientation, collisional electron spin relaxation, and chemical exchange. In the general physical situation, the electron spin relaxation rate,  $\tau_{S,p}^{(\mu)}$ , depends on spin eigenstate ( $\mu$ ) and on the spatial coordinate of spin decay ( $p = 0, \pm 1$ ) (Section 5 contains further discussion). In most applications, the electron spin relaxation rates are taken to be the eigenstate-averaged values,  $(\tau_{S,p})^{-1}$ , in which case the superscript ( $\mu$ ) is not needed in Eqs. (23a)–(23c).

The ensemble average (ea) is calculated over molecular orientations. Parelax2 implements this by averaging a set of 92 orientations where the polar angles of  $\hat{B}_0$  in the MF are specified by the polar angles of the 60

vertices and 32 face centers of the truncated icosahedron (buckeyball).

### 4.3. The MF “constant $H_S$ ” formulation

The MF formulation of the theory provides a more transparent description of physical situations in the vicinity of the zfs-limit, where the motion of  $S$  is spatially quantized (or polarized) along molecule-fixed axes. Starting from Eq. (10),  $B_{\pm 1}^{(1)}$  are transformed to the MF as

$$B_{\pm 1}^{(1)} = \sum_{q=-1}^{+1} \hat{B}_q^{(1)} D_{q,\pm 1}^{(1)}(\alpha, \beta, \gamma), \quad (24)$$

giving

$$R_{1M} = -\gamma_I^2 \int_{-\infty}^{+\infty} dt \exp(i\omega_I t) \text{Re} \left\{ \sum_{q,q'=-1}^1 \langle \hat{B}_q^{(1)}(t) \hat{B}_{q'}^{(1)}(0) \rangle_S \right. \\ \left. \times D_{q,+1}^{(1)}(\alpha, \beta, \gamma, t) D_{q',-1}^{(1)}(\alpha, \beta, \gamma, 0) \right\}_{\text{ea}}. \quad (25)$$

Using the component expressions for  $\hat{B}_{(1)}$  in Appendix B but with spin ( $\hat{S}_p^{(1)}$ ) and spatial variables ( $\hat{\theta}, \hat{\phi}$ ) defined in the MF, leads to the following expression for  $R_{1M}$ :

$$R_{1M} = -48\pi(\gamma_I g_e \beta_e)^2 r_{IS}^{-6} (\mu_0/4\pi)^2 \sum_{q,q'=-1}^1 \sum_{p,p'=-1}^1 \\ \times \left\{ \begin{matrix} 1 & 2 & 1 \\ p & (q-p) & -q \end{matrix} \right\} \left\{ \begin{matrix} 1 & 2 & 1 \\ p' & (q'-p') & -q' \end{matrix} \right\} \\ \times (-1)^{q+q'} Y_{q-p}^{(2)}(\hat{\theta}, \hat{\phi}) Y_{q'-p'}^{(2)}(\hat{\theta}, \hat{\phi}) \\ \times \left\{ D_{q,+1}^{(1)}(\alpha, \beta, \gamma) D_{q',-1}^{(1)}(\alpha, \beta, \gamma) \right. \\ \left. \times (2S+1)^{-1} \sum_{\mu, \nu} \langle \mu | \hat{S}_p^{(1)} | \nu \rangle \langle \nu | \hat{S}_{p'}^{(1)} | \mu \rangle \hat{j}_p(\omega_{\mu\nu})_{\text{ea}} \right\}, \quad (26a)$$

$$\hat{j}_p(\omega_{\mu\nu}) = \frac{\hat{\tau}_{d,p}}{1 + (\omega_I - \omega_{\mu\nu})^2 (\hat{\tau}_{d,p})^2}. \quad (26b)$$

The spin matrix elements in Eq. (26a) are evaluated in the eigensystem of  $H_S^0(\alpha, \beta, \gamma; t)$ , as in the LF formulation, but the spin components,  $\hat{S}_q^{(1)}$ , are defined with respect to the MF.

The dipolar correlation time,  $\hat{\tau}_{d,p}$ , is defined as follows:

$$(\hat{\tau}_{d,p})^{-1} = (\tau_R^{(1)})^{-1} + (\hat{\tau}_{S,p})^{-1} + (\tau_M)^{-1}, \quad (26c)$$

which differs from the dipolar correlation time of LF theory in two ways. First, the reorientational correlation time is that for a 1st-rank, rather than a 2nd-rank, molecule-fixed tensor, corresponding to the 1st-rank Wigner rotation matrix elements in Eq. (26a). These correlation

times are related as  $\tau_R^{(1)} = 3\tau_R^{(2)}$ . The fact that  $\tau_R^{(1)}$ , rather than  $\tau_R^{(2)}$ , appears in the MF formulation reflects the fact that the  $I$ - $S$  dipolar interaction transforms on molecular rotation as a vector when  $S$  is quantized in the MF [1]. It should be recognized, however, that the MF “constant  $H_S$ ” formulation does not give a very accurate description of the effects of Brownian motion in any regime of field strength, including the zfs-limit, because it ignores the effect of reorientation of the zfs tensor axes on electron spin relaxation, for which an accurate description requires SD. In practical analyses, we often omit  $\tau_R^{(1)}$  in Eq. (26c) and use Eq. (26a) as subject to a slow reorientation assumption.

The second difference in  $\tau_{d,p}$  and  $\hat{\tau}_{d,p}$  is in the electron spin relaxation times, which must be defined in the LF for the former and the MF for the latter (see Section 5). As in Eqs. (23a)–(23c), we take these quantities to be averaged over eigenstates.

#### 4.4. “Constant $H_S$ ” ZFS-limit theory [5]

This MF formulation is valid only in the zfs-limit, unlike the MF formulation of the previous section (Eqs. (26a)–(26c)), which is valid in all regimes of field strength. In the zfs limit, the spin motion is polarized along the zfs principal axes  $(\hat{x}, \hat{y}, \hat{z})$ , and the NMR-PRE depends on the orientation of the interspin vector,  $\vec{r}_{IS}$ , in the molecular frame. The “constant  $H_S$ ” zfs-limit formulation provides explicit functional forms for the angular dependence of  $R_{1M}$  on  $(\hat{\theta}, \hat{\phi})$ , the polar angles which specify the orientation of the  $I$ - $S$  interspin vector in the MF.

It has been shown [5] that in the zfs-limit,  $R_{1M}$  can be written as a sum of cartesian contributions,

$$R_{1M} = \sum R_{1r} \quad (r = \hat{x}, \hat{y}, \hat{z}) \quad (27a)$$

each of which contains the matrix elements of a single spin component,  $\langle \hat{S}_r \rangle$ :

$$R_{1r} = (8/3)(g_e \beta_e \gamma_I)^2 (\mu_0/4\pi)^2 r_{IS}^{-6} (2S+1)^{-1} \times [1 + P_2(\cos \hat{\theta}_r)] \sum_{\mu, \nu \geq \mu} |\langle \mu | \hat{S}_r | \nu \rangle|^2 \hat{J}_r(\omega_{\mu\nu}). \quad (27b)$$

Thus  $R_{1\hat{x}}$  depends only on  $\langle \hat{S}_x \rangle$ , etc. The function,  $[1 + P_2(\cos \hat{\theta}_r)]$ , describes the angular variation of the NMR-PRE with respect to nuclear spin position in the MF.  $P_2(\cos \hat{\theta}_r)$  is the 2nd-order Legendre polynomial, the argument of which is the direction cosine of  $\vec{r}_{IS}$  with respect to the  $r$ th zfs principal axis. The physical significance of these functions is that they describe the angular variation of the mean-square local field of a dipole moment (either classical or quantum mechanical) located at the origin and oriented along the  $r$ th cartesian axis (see Fig. 1) [5].

In most cases, the matrix elements,  $\langle \mu | \hat{S}_r | \nu \rangle$ , of specific spin components are responsible for the various well-

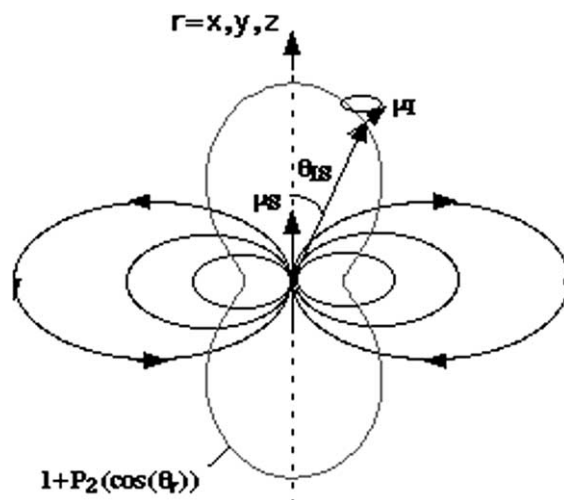


Fig. 1. Flux lines of a magnetic moment,  $\vec{\mu}_S$ , oriented along the  $r$ th cartesian axis are shown. A contour of the function,  $[1 + P_2(\cos \theta_{IS})]$ , which describes the angular variation of the mean-square local field at constant  $I$ - $S$  interspin distance, is also shown.

defined dispersive features in an MRD profile. The amplitudes of these features depend on nuclear orientation  $(\hat{\theta}_r)$  as described by Eqs. (27b). As a zfs-limit example for  $S=1$ , when the zfs tensor has cylindrical symmetry (i.e.,  $D \neq 0$ ,  $E=0$ ),  $\langle \hat{S}_z \rangle$  is a constant of the motion, and  $R_{1M} \approx R_{1z}$ . In this case,  $R_{1M}$  varies as  $[1 + P_2(\cos \hat{\theta}_z)]$  and is essentially independent of  $\hat{\theta}_x$  and  $\hat{\theta}_y$ . The dependence of  $R_{1M}$  on the orientation of  $\vec{r}_{IS}$  is as illustrated in Fig. 1 with  $r = \hat{z}$ . At fixed  $I$ - $S$  interspin distance, axial nuclear locations  $\hat{\theta}_z = 0$  are relaxed four times more efficiently than equatorial locations  $\hat{\theta}_z = \pi/2$ . An experimental example is discussed in [8].

For other spins and other zfs tensor symmetries,  $\langle \hat{S}_x \rangle$  and  $\langle \hat{S}_y \rangle$  may contribute significantly to  $R_{1M}$ . The transverse spin components are usually not constants of the motion. These contributions often produce well defined dispersive features, the amplitudes of which are proportional to  $[1 + P_2(\cos \hat{\theta}_x)]$  and  $[1 + P_2(\cos \hat{\theta}_y)]$ . An experimental example involving the  $S=3/2$  ion, Co(II), is discussed in [9].

## 5. The collisional electron spin relaxation mechanism

The collisional electron spin relaxation mechanism (i.e., that due to  $H_{zfs}^c(t)$  in Eq. (16)) involves some subtleties which require further discussion. This mechanism has traditionally been described by the Zeeman-limit BM theory [28]. As described in Section 3, Parelax2 provides this as one option. Another option is provided which calculates  $\tau_S$  using theory [44,48], which incorporates the hamiltonian of Eqs. (20a) and (20b). The spin TCF in Eq. (14) can be written

$$\begin{aligned}
G_{p,p'}(t) &= (2S + 1)^{-1} \text{Tr} \left[ U^\dagger(t) S_p^{(1)} U(t) S_{p'}^{(1)} \right], \quad (28a) \\
&= (2S + 1)^{-1} \sum_{\mu} \exp(-t/\tau_{S,p}^{(\mu)}) \\
&\quad \times \left\langle \mu \left| \exp(iH_S^0 t/\hbar) S_p^{(1)} \exp(-iH_S^0 t/\hbar) S_{p'}^{(1)} \right| \mu \right\rangle. \quad (28b)
\end{aligned}$$

From Eqs. (28b),  $\tau_{S,p}^{(\mu)}$ , describes the thermal decay of the  $\mu$ th matrix element of the trace. These eigenstate-specific quantities, for which expressions have been derived in terms of Redfield matrix elements [48], are appropriate for use in the LF “constant  $H_S$ ” formulation (Eqs. (23a)). For example, the term in Eq. (23a) which contains the matrix element,  $\langle \mu | S_p^{(1)} | \nu \rangle$ , requires an associated spectral density function,  $J_p^{(\mu)}(\omega_{\mu\nu})$ , calculated using the eigenstate-specific decay constant,  $\tau_{S,p}^{(\mu)}$ .

The use of eigenstate-specific decay constants is overly complex for most applications. What is needed is a description of electron spin relaxation that is comparable in complexity to BM Theory (i.e., two magnetic field-dependent electron spin relaxation times,  $\tau_{S1,2}$ , determined by two physical parameters,  $\Delta_i^2$  and  $\tau_v$ ) but which accounts for the effects of  $H_{zfs}^0(\alpha, \beta, \gamma)$ . This is provided by decay constants,  $\tau_{S,r}$ , which are averaged over spin eigenstates. Sharp [44] gives the following expressions for these quantities:

$$\begin{aligned}
(\tau_{S,r})^{-1} &= [S(S + 1)/3]^{-1} (2S + 1)^{-1} (\Delta_i^2/5) \\
&\quad \times \left\{ \sum_q n_q^{(r)} \sum_{\mu,\nu} \left| \langle \mu | S_q^{(2)} | \nu \rangle \right|^2 k(\omega_{\mu\nu}) \right\}_{\text{ea}}, \quad (29a)
\end{aligned}$$

$$k(\omega) = \tau_v / (1 + \omega^2 \tau_v^2). \quad (29b)$$

The  $S_q^{(2)}$  in Eq. (29a) are the five quadratic cartesian tensor functions of the spin operators which transform spatially like the d-orbitals ( $q=1-5$  correspond to  $z^2$ ,  $x^2 - y^2$ ,  $xz$ ,  $yz$ ,  $xy$ ). The quantities,  $n_q^{(r)}$ , are integer coefficients which arise in a calculation of the double commutators of the spin operators [44]. The matrix elements are evaluated in the eigenbasis,  $\mu, \nu$ , of  $H_S^0(\alpha, \beta, \gamma)$ , and  $\Delta_i$  has units of  $\text{rad s}^{-1}$ .

The relaxation times,  $\tau_{S,r}$ , are suitable for use in the LF formulations of theory (i.e., SD simulation and the LF “constant  $H_S$ ” formulation). These quantities are analogous to the relaxation times,  $\tau_{S1,2}$ , of BM Theory but account for the effects of  $H_{zfs}^0$ , which may have any magnitude or symmetry. Two physical parameters,  $\Delta_i$  and  $\tau_v$ , are required for the calculation as in BM Theory.

### 5.1. LF versus MF formulations

The MF formulations require a different set of relaxation times, namely,  $\hat{\tau}_{S,r}^{(\mu)}$  or  $\hat{\tau}_{S,r}$ , describing the decay of spin TCF's,  $\hat{G}_{p,p'}(t)$ , along molecule-fixed axes. These decay constants can be calculated using expressions analo-

gous to Eqs. (29a) and (29b) but cast in the molecular frame; in particular, the matrix elements of the MF spin operators,  $\hat{S}_q^{(2)}$ , are needed instead of the LF spin operators,  $S_q^{(2)}$ . Parelax2 carries out the LF and MF calculations separately. In the first step,  $H_S^0(\alpha, \beta, \gamma)$  is formulated in the desired coordinate frame, either LF or MF. Then  $H_S^0(\alpha, \beta, \gamma)$  is diagonalized, and the spin matrix elements are calculated,  $\langle \mu | S_q^{(2)} | \nu \rangle$  for the LF calculation and  $\langle \mu | \hat{S}_q^{(2)} | \nu \rangle$  for the MF calculation. In both calculations, the spin matrix elements are evaluated in the eigenbasis of  $H_S^0(\alpha, \beta, \gamma)$ . Both sets of electron spin relaxation times,  $\tau_{S,r}$  ( $r = x, z$ ) and  $\hat{\tau}_{S,r}$  ( $r = \hat{x}, \hat{y}, \hat{z}$ ), are calculated in each physical situation. The LF decay constants are used in the LF formulations (SD and LF “constant  $H_S$ ”), and the MF decay constants are used in the MF formulations (MF “constant  $H_S$ ” and zfs-limit “constant  $H_S$ ”).

Complications due to effects of molecular anisotropy arise in the MF calculation of  $\hat{\tau}_{S,r}$  that are absent in the LF calculation. In many practical cases, these effects can be ignored, but we give a brief account of them. The contribution of each quadratic degree of freedom to  $\hat{\tau}_{S,r}$  depends on a mean-square zfs coupling constant,  $c_q^2$ , and a correlation time,  $\tau_v^{(q)}$ , which in general differ for different  $q$ . In metalloporphyrins, for example,  $q = 2$  ( $\hat{x}^2 - \hat{y}^2$ ) has quite different dynamical and electronic properties than  $q = 1$  ( $\hat{z}^2$ ). In general, five distinct values of  $c_q^2$  and  $\tau_v^{(q)}$  are needed for the anisotropic case. Also, there is a cross term between  $\hat{z}^2$  and  $\hat{x}^2 - \hat{y}^2$  in the MF form of Eqs. (29a) and (29b) (it vanishes in the LF) which is in general non-zero when  $H_{zfs}^0$  contains low symmetry terms [44]. Parelax2 can carry out these calculations, but this involves increased complexity in the physical parameterization, which is usually not warranted in experimental studies. When molecular anisotropy is neglected, a single zfs parameter,  $\Delta_i^2 = 5c_q^2$ , is needed as in BM Theory.

These effects of molecular anisotropy do not arise in LF calculations, since spin decay along laboratory axes in a powder is uncorrelated with the zfs tensor orientation.

### 5.2. Limiting behavior

The limiting behavior of  $\tau_{S,r}$  and  $\hat{\tau}_{S,r}$  has some interesting aspects. In the Zeeman-limit, the LF quantities ( $\tau_{S,z}$ ,  $\tau_{S,x}$ ) are equal to the BM quantities ( $\tau_{S1,2}$ ) as expected. However the MF quantities,  $\hat{\tau}_{S,r}$ , do not; rather, the average MF relaxation rate approaches the average LF relaxation rate; i.e.,

$$(\hat{\tau}_{S,z})^{-1} = (\hat{\tau}_{S,x})^{-1} = (\hat{\tau}_{S,y})^{-1} = 3^{-1} (\tau_{S1}^{-1} + 2\tau_{S2}^{-1}).$$

That the MF polarizations are equivalent in the Zeeman-limit ( $\hat{x} = \hat{y} = \hat{z}$ ) reflects the fact that the molecular axes are uncorrelated with  $H_{Z\text{cem}}$ .



In the zfs-limit, there are three distinct MF relaxation times ( $r = \hat{x}, \hat{y}, \hat{z}$ ) when  $H_{zfs}^0$  has orthorhombic symmetry and two when  $H_{zfs}^0$  is cylindrical. In this limit, the laboratory axes are uncorrelated with the spin motion, and the LF relaxation rates approach the average of the MF relaxation rates

$$(\tau_{S,z})^{-1} = (\tau_{S,x})^{-1} = 3^{-1}(\hat{\tau}_{Sx}^{-1} + \hat{\tau}_{Sy}^{-1} + \hat{\tau}_{Sz}^{-1}).$$

## 6. Discussion

It should be noted that the LF and MF “constant  $H_S$ ” formulations of Sections 4.2 and 4.3 are not limiting expressions valid only in the Zeeman and zfs-limits, respectively. Rather, both formulations are valid in all regimes of field strength, providing that electron spin relaxation is treated equivalently, i.e., when all electron spin relaxation times for all spatial polarizations in both MF and LF have the same numerical value. Physically, this occurs when  $\tau_v$  is very short. Since the average value of the  $\tau_{S,r}$  ( $r = x, z$ ) equals that of the  $\hat{\tau}_{S,r}$  ( $r = \hat{x}, \hat{y}, \hat{z}$ ), it also occurs when electron spin relaxation is isotropic in both the LF and MF. When this is not true, the LF and MF formulations give different results for  $R_{1M}$ .

The principal rationale for using both LF and MF formulations involves physical transparency. When the coordinate frame matches the spatial quantization of the spin motion (but not otherwise), the spin matrix elements are readily interpretable physically. In the Zeeman-limit, for example,  $\langle S_z \rangle$  is a constant of the motion, and  $\langle S_x \rangle$  oscillates at the Larmor frequency. The contributions of the LF spin matrix elements in Eq. (23a) are readily interpretable since the associated spectral density functions, which describe the power density of the dipolar field, are evaluated at spin eigenfrequencies. The MF quantities,  $\langle \hat{S}_z \rangle$  and  $\langle \hat{S}_x \rangle$ , in Eq. (26a) are not so readily interpretable, since the Zeeman-limit spin motion is not quantized along molecular axes. Of course, the converse is true in the vicinity of the zfs-limit, where the MF description is physically informative but the LF description is not. In all regimes of field strength, however, both LF and MF formulations give identical numerical results for  $R_{1M}$  as long as electron spin relaxation is treated equivalently.

## Acknowledgment

This material is based upon work supported by the National Science Foundation under Grant No. CHE-0209616.

## Appendix A. Spherical tensor form of the $I$ - $S$ dipole-dipole hamiltonian in SI units

$$H_{IS} = - \left( \frac{6\pi}{5} \right)^{1/2} \left( \frac{\gamma_I g_e \beta_e}{r_{IS}^3} \right) \left( \frac{\mu_0}{4\pi} \right) (A + C + D + E + F), \quad (\text{A.1})$$

$$A = 2 \cdot 6^{-1/2} \left( 2I_0^{(1)} S_0^{(1)} + I_{+1}^{(1)} S_{-1}^{(1)} + I_{-1}^{(1)} S_{+1}^{(1)} \right) Y_0^{(2)}(\theta, \phi), \quad (\text{A.2})$$

$$C = -2^{1/2} \left( I_{+1}^{(1)} S_0^{(1)} + I_0^{(1)} S_{+1}^{(1)} \right) Y_{-1}^{(2)}(\theta, \phi), \quad (\text{A.3})$$

$$D = -2^{1/2} \left( I_{-1}^{(1)} S_0^{(1)} + I_0^{(1)} S_{-1}^{(1)} \right) Y_{+1}^{(2)}(\theta, \phi), \quad (\text{A.4})$$

$$E = +2 \left( I_{+1}^{(1)} S_{+1}^{(1)} \right) Y_{-2}^{(2)}(\theta, \phi), \quad (\text{A.5})$$

$$F = +2 \left( I_{-1}^{(1)} S_{-1}^{(1)} \right) Y_{+2}^{(2)}(\theta, \phi). \quad (\text{A.6})$$

**Appendix B. Spherical tensor components,  $B_m^{(1)}$ , of the dipolar field operator,  $B_{(1)}$ , defined in Eq. (6b) of the text. The spatial arguments,  $\theta$ ,  $\varphi$ , of  $B_m^{(1)}(\theta, \varphi)$ , and  $Y_q^{(2)}(\theta, \varphi)$  are omitted for brevity**

$$B_{+1}^{(1)} = c_B 3^{1/2} \left( 30^{-1/2} S_{+1}^{(1)} Y_0^{(2)} - 10^{-1/2} S_0^{(1)} Y_{+1}^{(2)} + 5^{-1/2} S_{-1}^{(1)} Y_{+2}^{(2)} \right), \quad (\text{B.1})$$

$$B_0^{(1)} = -c_B 3^{1/2} \left( -10^{-1/2} S_{+1}^{(1)} Y_{-1}^{(2)} + 2^{1/2} 15^{-1/2} S_0^{(1)} Y_0^{(2)} - 10^{-1/2} S_{-1}^{(1)} Y_{+1}^{(2)} \right), \quad (\text{B.2})$$

$$B_{-1}^{(1)} = c_B 3^{1/2} \left( 5^{-1/2} S_{+1}^{(1)} Y_{-2}^{(2)} - 10^{-1/2} S_0^{(1)} Y_{-1}^{(2)} + 30^{-1/2} S_{-1}^{(1)} Y_0^{(2)} \right), \quad (\text{B.3})$$

$$c_B = -g_e \beta_e r_{IS}^{-3} (8\pi)^{1/2} (\mu_0/4\pi). \quad (\text{B.4})$$

## References

- [1] R.R. Sharp, Effect of zero field splitting interactions on the paramagnetic relaxation enhancement of nuclear spin relaxation rates in solution, *J. Chem. Phys.* 98 (1993) 912–921.
- [2] R.R. Sharp, Characteristic properties of the nuclear magnetic resonance-paramagnetic relaxation enhancement arising from integer and half-integer electron spins, *J. Chem. Phys.* 98 (1993) 2507–2515.
- [3] R.R. Sharp, Nuclear spin relaxation due to paramagnetic species in solution: effect of anisotropy in the zero field splitting tensor, *J. Chem. Phys.* 98 (1993) 6092–6101.
- [4] J.-M. Bovet, R.R. Sharp, Nuclear magnetic resonance relaxation enhancements produced by paramagnetic solutes: effects of

- rhombicity in the zero field splitting tensor with the  $S=2$  spin system as an example, *J. Chem. Phys.* 99 (1993) 18–26.
- [5] R. Sharp, S.M. Abernathy, L.L. Lohr, Paramagnetically induced nuclear magnetic resonance relaxation in solutions containing  $S > 1$  ions: a molecular-frame theoretical and physical model, *J. Chem. Phys.* 107 (1997) 7620–7629.
- [6] S.M. Abernathy, J.C. Miller, L.L. Lohr, R.R. Sharp, Nuclear magnetic resonance-paramagnetic relaxation enhancements: influence of spatial quantization of the electron spin when the zero-field splitting energy is larger than the Zeeman energy, *J. Chem. Phys.* 109 (1998) 4035–4046.
- [7] J.C. Miller, R.R. Sharp, Paramagnetic NMR relaxation enhancement: spin dynamics simulations of the effect of zero-field splitting interactions for  $S = 5/2$ , *J. Phys. Chem. A* 104 (2000) 4889–4895.
- [8] J. Miller, S. Abernathy, R. Sharp, NMR paramagnetic relaxation enhancement: measurement of an axial/equatorial  $T_1$  ratio for  $S=1$  in the zero-field splitting limit, *J. Phys. Chem. A* 104 (2000) 4839–4845.
- [9] J.C. Miller, S.M. Abernathy, L.L. Lohr, R.R. Sharp, NMR paramagnetic relaxation enhancement: ZFS-limit behavior for  $S = 3/2$ , *J. Phys. Chem. A* 104 (2000) 9481–9488.
- [10] J.C. Miller, L.L. Lohr, R.R. Sharp, NMR paramagnetic relaxation enhancement: test of the controlling influence of ZFS rhombicity for  $S = 1$ , *J. Magn. Reson.* 148 (2001) 267–276.
- [11] N. Schaeffe, R. Sharp, NMR paramagnetic relaxation due to the  $S = 5/2$  complex, Fe(III)-TSPP: central role of the tetragonal 4th-order ZFS interaction, *J. Chem. Phys.* 122 (2005) 184501–184511.
- [12] N. Schaeffe, R. Sharp, NMR-paramagnetic relaxation due to the high-spin  $d^3$  electron configuration: Cr<sup>III</sup>-TSPP, *J. Phys. Chem. A* 109 (2005) 3276–3284.
- [13] N. Schaeffe, R. Sharp, NMR paramagnetic relaxation of the spin 2 complex Mn(III)TSPP: a unique mechanism, *J. Phys. Chem. A* 109 (2005) 3267–3275.
- [14] T. Nilsson, J. Kowalewski, Slow-motion theory of nuclear spin relaxation in paramagnetic low-symmetry complexes: a generalization to high electron spin, *J. Magn. Reson.* 146 (2000) 345–358.
- [15] T. Nilsson, J. Kowalewski, Low-field theory of nuclear spin relaxation in paramagnetic low symmetry complexes for electron spin systems of  $S = 1, 3/2, 2, 5/2, 3$  and  $7/2$ , *Mol. Phys.* 98 (2000) 1617–1638.
- [16] J. Svoboda, T. Nilsson, J. Kowalewski, P.-O. Westlund, P.T. Larsson, Field-dependent proton NMR relaxation in aqueous solutions of Ni(II) ions. A new interpretation, *J. Magn. Reson. A* 121 (1996) 108–113.
- [17] D. Kruk, T. Nilsson, J. Kowalewski, Nuclear spin relaxation in paramagnetic systems with zero-field splitting and arbitrary electron spin, *Phys. Chem. Phys.* 3 (2001) 4907–4917.
- [18] H. Fukui, K. Miura, H. Matsuda, The rhombic effect of zero-field splitting on the nuclear relaxation times. Quenching of the electron spin angular momentum, *J. Magn. Reson.* 88 (1990) 311.
- [19] T. Nilsson, J. Svoboda, P.-O. Westlund, J. Kowalewski, Slow-motion theory of nuclear spin relaxation in paramagnetic complexes ( $S = 1$ ) of arbitrary symmetry, *J. Chem. Phys.* 109 (1998) 6364–6375.
- [20] S.M. Abernathy, R.R. Sharp, Spin dynamics calculations of electron and nuclear spin relaxation times in paramagnetic solutions, *J. Chem. Phys.* 106 (1997) 9032–9043.
- [21] J.C. Miller, N. Schaeffe, R.R. Sharp, Calculating NMR paramagnetic relaxation enhancements without adjustable parameters: the spin-3/2 complex Cr(III)(AcAc)<sub>3</sub>, *Magn. Reson. Chem.* 41 (2003) 806–812.
- [22] N. Schaeffe, R. Sharp, Electron spin relaxation due to reorientation of a permanent zero field splitting tensor, *J. Chem. Phys.* 121 (2004) 5387–5394.
- [23] R.R. Sharp, Nuclear-spin relaxation in paramagnetic solutions when the electronic zero-field splitting and zeeman interactions are of arbitrary magnitude, *J. Magn. Reson.* 100 (1992) 491–516.
- [24] I. Bertini, O. Galas, C. Luchinat, G. Parigi, A computer program for the calculation of paramagnetic enhancements of nuclear-relaxation rates in slowly rotating systems, *J. Magn. Reson. A* 113 (1995) 151–158.
- [25] Z. Luz, S. Meiboom, Proton relaxation in dilute solutions of cobalt(II) and nickel(II) ions in methanol and the rate of methanol exchange of the solvation sphere, *J. Chem. Phys.* 40 (1964) 2686–2692.
- [26] I. Solomon, Relaxation processes in a system of two spins, *Phys. Rev.* 99 (1955) 555–565.
- [27] N. Bloembergen, Proton relaxation times in paramagnetic solutions, *J. Chem. Phys.* 27 (1957) 572–573, Comment on “Proton relaxation times in paramagnetic solutions”, *J. Chem. Phys.* 27 (1957) 595–596..
- [28] N. Bloembergen, L.O. Morgan, Proton relaxation times in paramagnetic solutions. Effects of electron spin relaxation, *J. Chem. Phys.* 34 (1961) 842–850.
- [29] R. Kubo, K. Tomita, A general theory of magnetic resonance absorption, *J. Phys. Soc. Jpn.* 9 (1954) 888–919.
- [30] L. Banci, I. Bertini, C. Luchinat, Nuclear and electron relaxation, VCH Publishers, Weinheim, 1991, pp. 185–191..
- [31] S.A. Altshuler, K.A. Valiev, On the theory of longitudinal relaxation of paramagnetic salt solutions, *Zh. Eksp. Teor. Fiz.* 35 (1958) 947–958, [English translation: *Sov. Phys. JETP* 8 (1959) 661–668].
- [32] D. Kruk, J. Kowalewski, Vibrational motions and nuclear spin relaxation in paramagnetic complexes: hexa-aqua-nickel(II) as an example, *J. Chem. Phys.* 116 (2002) 4079–4086.
- [33] D. Kruk, J. Kowalewski, P.-O. Westlund, Nuclear and electron spin relaxation in paramagnetic complexes in solution: effects of the quantum nature of molecular vibrations, *J. Chem. Phys.* 121 (2004) 2215–2227.
- [34] M. Odelius, C. Ribbing, J. Kowalewski, Spin dynamics under the Hamiltonian varying with time in discrete steps: molecular dynamics-based simulation of electron and nuclear spin relaxation in aqueous nickel(II), *J. Chem. Phys.* 104 (1996) 3181–3188.
- [35] M. Odelius, C. Ribbing, J. Kowalewski, Molecular dynamics simulation of the zero-field splitting fluctuations in aqueous Ni(II), *J. Chem. Phys.* 103 (1995) 1800–1811.
- [36] P.-O. Westlund, N. Benetis, H. Wennerstroem, Paramagnetic proton nuclear magnetic relaxation in the nickel(2+) hexa-aqua complex. A theoretical study, *Mol. Phys.* 61 (1987) 177–194.
- [37] P.-O. Westlund, P.T. Larsson, Proton-enhanced relaxation in low-symmetry paramagnetic complexes ( $S = 1$ ): beyond the Solomon-Bloembergen and Morgan theory. 1. The Smoluchowsky distortion model of the ZFS interaction, *Acta Chem. Scand.* 45 (1991) 11–18.
- [38] T. Larsson, P.-O. Westlund, J. Kowalewski, S.H. Koenig, Nuclear-spin relaxation in paramagnetic complexes in the slow-motion regime for the electron spin: the anisotropic pseudorotation model for  $S = 1$  and the interpretation of nuclear magnetic relaxation dispersion results for a low-symmetry Ni(II) complex, *J. Chem. Phys.* 101 (1994) 1116–1128.
- [39] S. Rast, P. Fries, E. Belorizky, A. Borel, L. Helm, A.E. Merbach, A general approach to the electronic spin relaxation of Gd(III) complexes in solutions. Monte Carlo simulations beyond the Redfield limit, *J. Chem. Phys.* 115 (2001) 7554–7563.
- [40] P.-O. Westlund, A low-field paramagnetic nuclear spin relaxation theory, *J. Chem. Phys.* 108 (1998) 4945–4953.
- [41] I. Bertini, J. Kowalewski, C. Luchinat, T. Nilsson, G. Parigi, Nuclear spin relaxation in paramagnetic complexes of  $S = 1$ : electron spin relaxation effects, *J. Chem. Phys.* 111 (1999) 5795–5807.

- [42] S. Rast, P.H. Fries, E. Belorizky, Static zero field splitting effects on the electronic relaxation of paramagnetic metal ion complexes in solution, *J. Chem. Phys.* 113 (2000) 8724–8735.
- [43] S. Rast, A. Borel, L. Helm, E. Belorizky, P.H. Fries, A.E. Merbach, EPR spectroscopy of MRI-related Gd(III) complexes: simultaneous analysis of multiple frequency and temperature spectra, including static and transient crystal field effects, *J. Am. Chem. Soc.* 123 (2001) 2637–2644.
- [44] R. Sharp, Closed-form expressions for level-averaged electron spin relaxation times outside the Zeeman limit: application to paramagnetic NMR relaxation, *J. Magn. Reson.* 154 (2002) 269–279.
- [45] E.N. Ivanov, Theory of rotational Brownian motion, *Zh. Eksp. Teor. Fiz.* 45 (1963) 1509–1517, [English translation: *Sov. Phys. JETP* 18 (1964) 1041–1045].
- [46] A. Messiah, *Quantum Mechanics*, Wiley, New York, 1962, Chapter XVII.
- [47] S.M. Blinder, *Foundations of Quantum Mechanics*, Academic Press, New York, 1974 (Chapter 7).
- [48] R. Sharp, L. Lohr, Thermal relaxation of electron spin motion in a thermal equilibrium ensemble: relation to paramagnetic nuclear magnetic resonance relaxation, *J. Chem. Phys.* 115 (2001) 5005–5014.